

Hydrogen co-firing simulation for emission reduction and efficiency in an 880 MW combined cycle power plant

Eka Octaviyatna Mulyadi, Praswasti PDK Wulan*

Engineering Faculty, University of Indonesia, Depok 16425,
Indonesia

*Corresponding Author: praswasti.pembangun@ui.ac.id

Abstract

This study evaluates the environmental and performance impacts of hydrogen co-firing with natural gas in an 880 MW Combined Cycle Power Plant (CCPP) in Jakarta, Indonesia. CO₂ emissions were estimated using the IPCC Tier-2 Method, while the Aspen Plus[®] simulation analyzed combustion performance under 10% and 20% hydrogen blending. Fuel composition was determined through Gas Chromatography analysis and processed using a weighted average method. The results show that hydrogen blending significantly reduces CO₂ emissions to approximately 10% at 10% hydrogen and 20% at 20% hydrogen, equivalent to 409420 tons annually. NO_x emissions increased moderately, by about 2.16% at 20% hydrogen, due to higher flame temperatures, yet remained far below the regulatory limit of 400 mg/Nm³. Thermal efficiency improved from 54.08% (baseline) to 56.88% and 60.06% with 10% and 20% hydrogen, respectively, although net power output slightly declined. These findings highlight the role of hydrogen as a transitional energy carrier, capable of decarbonizing gas-fired power plants while improving efficiency with manageable environmental trade-offs. Although the study is based on steady-state simulations without pilot-scale validation, the integration of actual operational data strengthens its applicability. Hydrogen co-firing presents a technically viable pathway for reducing CO₂ emissions in the power sector.

Keywords:

Hydrogen co-firing, CO₂ emissions, gas power plant, thermal efficiency, NO_x emissions

1 Introduction

Indonesia's electricity demand is projected to increase significantly, driven by population growth and economic development [1]. While fossil fuels, particularly coal, still dominate the energy mix, there is a push towards renewable energy sources [2]. The government aims to increase renewable energy in the national energy mix, but progress has been slow [3]. Studies show that non-renewable energy consumption and Carbon Dioxide (CO₂) emissions positively impact economic growth, while renewable energy's effect is not yet substantial [4], [5]. The Environmental Kuznets Curve hypothesis is not valid for CO₂ emissions in Indonesia, suggesting emissions will continue to rise with income [6]. Multiple factors drive coal consumption, including energy mix changes, urbanization, and income growth [7]. Transitioning to renewable energy and reducing fossil fuel dependence are crucial for environmental sustainability and meeting climate goals.

The use of natural gas in Combined Cycle Gas and Steam Power Plants (CCPPs) has reached a high maturity level as an energy source due to its ability to provide stable performance and low operational costs. CCPP is often chosen as a transitional solution to clean energy

because the supporting infrastructure is already available, and this technology is easily integrated into modern power generation systems [8]. Hydrogen is seen as a potential solution for the future due to its ability to reduce carbon emissions significantly. In addition to being relevant in the power generation sector, hydrogen also has wide applications in the transportation sector, such as in fuel cell vehicles and industrial heating systems, all of which support decarbonization efforts across various sectors [9]. Hydrogen has several key advantages, including the absence of carbon emissions when burned, with water as the only byproduct, making it an environmentally friendly fuel and ideal for supporting a clean energy future [10]. Additionally, hydrogen has a high energy density, allowing for large-scale energy storage, and can be used as an energy vector to balance supply and demand in renewable energy-based electricity grids [11]. According to Rieksta et al, the global energy transition shows a significant shift from fossil energy sources, such as oil and coal, towards renewable energy, with hydrogen projected as the primary fuel of the future to support energy sustainability and carbon emission reduction [11].

Co-firing has emerged as an attractive and innovative solution, where natural gas can be used in conjunction with alternative hydrogen fuel. Co-firing is a method in which two or more fuel types are used simultaneously in a power plant to improve efficiency and reduce Greenhouse Gas (GHG) emissions [12]. This technology enables the flexible and efficient use of various fuels without replacing existing infrastructure, thereby supporting the sustainability of power plant operations [13].

The application of hydrogen co-firing with natural gas in a Combined Cycle Gas Turbine and Steam Power Plant (CCGT) can significantly reduce GHG emissions without requiring the replacement of existing infrastructure. Gas turbines' flexibility in using hydrogen as a fuel, including fuels with high H₂ content, allows for seamless integration with the existing power plant infrastructure without requiring significant changes to the system design [14]. The selection of CCPP as the subject of this study is based on its high thermal efficiency, operational flexibility, and compatibility with hydrogen as a supplementary fuel. CCPP systems are widely used in Indonesia and can adapt to low-carbon fuels without major modifications, making them an ideal candidate for energy transition strategies. Hydrogen co-firing in CCPP allows for significant CO₂ emissions reduction while leveraging existing natural gas infrastructure, aligning with national decarbonization and energy diversification goals. Therefore, investigating hydrogen-natural gas co-firing in CCPP is both timely and technically sound within Indonesia's energy transition [15].

Despite the rising global attention on hydrogen co-firing, there remains a significant research gap in the Indonesian context, particularly concerning its quantified impact on emissions and operational performance in existing CCPPs. Most available studies have been conducted in developed countries with different regulatory, infrastructural, and energy system contexts. Moreover, research specifically targeting large-scale power plants, such as those with a capacity of 880 MW, is notably scarce, although these high-capacity facilities contribute substantially to Indonesia's electricity supply. To address this gap, the present study uses simulation-based analysis to evaluate the environmental emission impacts of hydrogen and natural gas co-firing in a large-scale, 880 MW CCPP. This analysis is further strengthened by using real operational parameters and actual fuel composition data from an operating Indonesian CCPP unit, enhancing the reliability and applicability of the results to current national conditions. The findings offer a comprehensive understanding of the emission reduction potential and environmental benefits associated with integrating hydrogen into Indonesia's existing gas and steam power infrastructure.

The objectives of this study are threefold: (1) to assess the reduction of CO₂ emissions through 10% and 20% hydrogen co-firing scenarios, (2) to evaluate the change in other key pollutants

such as NO_x, and (3) to analyze the resulting changes in thermal efficiency and fuel utilization using the Aspen Plus® simulation. These insights aim to inform Indonesia's transition to a cleaner, hydrogen-compatible power sector and provide evidence-based support for integrating hydrogen into national decarbonization strategies.

2 Methodology

This study employs both descriptive and quantitative methods. The descriptive approach involves a literature review of emission calculation theories. At the same time, the quantitative method uses historical data from the operation of an 880 MW CCPP. It simulates hydrogen blending scenarios from 0% to 20%. The main objective is to evaluate the impact of hydrogen blending on emissions and plant efficiency.

The study begins with formulating the research problem, which centers on using hydrogen as an alternative fuel to reduce GHG emissions and enhance the performance of power plants. This is followed by an extensive literature review to understand the current state of hydrogen co-firing technologies and their environmental implications. During the data collection phase, proximate and ultimate analyses, as well as gas chromatography, are employed to characterize the composition of the natural gas used in the power plant. Using the collected data, simulation modeling is conducted with Aspen Plus® under three different hydrogen blending scenarios: 0%, 10%, and 20% by volume. These simulations assess the resulting emission profiles, thermal performance, and overall plant efficiency under each blending condition.

Finally, the analysis of results compares the output from each scenario, emphasizing the reduction in CO₂ emissions and the increase in thermal efficiency. The findings provide insight into the environmental and operational implications of implementing hydrogen co-firing in CCPPs.

2.1 Emission calculation process

Based on the composition data of natural gas available throughout 2024 (as presented in Table 1), the carbon content (C) was calculated using a weighted average method, reflecting each component's proportion and its respective carbon contribution.

Table 1. Annual gas usage in 2024

Month	Unit	Gas turbine #1	Gas turbine #2	Monthly total
January		1242785.00	1682240.27	2925025.27
February		1482343.31	1544674.16	3027017.47
March		1297098.73	1818113.34	3115212.07
April		1074046.02	1146120.53	2220166.55
May		0	1877750.90	1877750.90
June	MMBTU	1159265.30	1395769.04	2555034.34
July		1697910.61	1530149.46	3228060.07
August		1727414.47	1483642.56	3211057.04
September		1527666.19	1660099.47	3187765.67
October		1636433.62	1689075.33	3325508.97
November		1572238.90	1499338.70	3071577.61
December		1525298.69	1580738.76	3106037.46
Total			34850213.42	

Combined with the Net Calorific Value (NCV), this value was used to estimate annual CO₂ emissions using the IPCC Tier 2 method, which considers the fuel's chemical properties and consumption. The calculation is expressed as Eq. (1).

$$E_{CO_2} = F_{gas} \times 0.001055 \times \frac{C}{NCV} \times FO \times 10^3 \times 44/12 \quad (1)$$

where E_{CO_2} is total CO₂ emissions (tons/year), F_{Gas} is net gas consumption (MMBTU), FO is oxidation factor, NCV is net calorific value (TJ/Gg), C is carbon content (%), and 0.001055 is conversion factor (MMBTU to TJ)

The emission analysis was conducted for three hydrogen blending scenarios: 0%, 10%, and 20%. Due to the challenge of direct emission measurement under varying combustion conditions, Aspen Plus® was used to simulate the co-firing process in a CCPP.

This allowed for more accurate modelling of CO₂ reductions and thermal system behavior.

For NO_x and SO₂ emissions, no direct emission calculation or measurement was conducted in this study. In practice, NO_x and SO₂ values are monitored using a Continuous Emissions Monitoring System (CEMS) in units of mg/Nm³. Therefore, the purpose of this study is limited to observing the potential trend of NO_x and SO₂ behavior, whether increasing or decreasing, under hydrogen co-firing scenarios (10% and 20%), as compared to the baseline condition with 100% natural gas. These insights are derived from the simulated combustion temperature and fuel composition rather than from explicit numerical prediction.

2.2 Simulation using Aspen Plus®

This study modelled the CCPP system using Aspen Plus® software. Aspen was chosen because it can accurately simulate thermodynamic processes, especially for natural gas-based power generation systems with varying fuel compositions. The system was modeled under steady-state conditions to analyze thermal efficiency, CO₂ emissions, and plant performance across different hydrogen blending scenarios. A schematic diagram of the CCPP system is shown in Fig. 1.

The modeling used operational data from the CCPP, including fuel consumption, pressure, temperature, and mass flow rates at various points in the system. The main components simulated include the gas turbine, Heat Recovery Steam Generator (HRSG), condenser, pump, compressor, and generator. To ensure the model's reliability, simulation results for the 100% natural gas (baseline) scenario were compared with actual operational data from the power plant. Parameters such as power output, exhaust gas temperature, and fuel consumption were used for validation. Once a good agreement with real operating conditions was confirmed, the model was applied to simulate hydrogen co-firing scenarios with confidence. A Gibbs Reactor was employed to model the combustor, enabling detailed simulation of the combustion process involving natural gas and hydrogen. Component selection and input data were based on the actual design characteristics of the CCPP, including fuel specifications analyzed through Gas Chromatography.

The simulation involved the combustion of natural gas and hydrogen in the gas turbine, adjusting operational parameters according to hydrogen blending scenarios (0%, 10%, 20%), and calculating outputs such as plant efficiency and CO₂ emissions. The Peng-Robinson fluid package was used to accurately represent the thermodynamic properties of the natural gas-hydrogen mixture. After completing the simulation, the output data were utilized for techno-economic analysis and environmental impact assessments of hydrogen co-firing implementation in the CCPP. The power plant efficiency in this study was calculated by comparing the total electrical energy produced with the total energy input consumed.

3 Results and discussion

3.1 Gas chromatography analysis data collection

This study aims to calculate the reduction in CO₂ emissions resulting from the co-firing of hydrogen with natural gas in a gas power plant. In this analysis, measurements are taken using the weighted average method, which is used to obtain more accurate values for carbon content and NCV [16]. The data obtained from these calculations are then used as the basis for estimating CO₂ emissions to evaluate the impact of co-firing on carbon emission reduction compared to pure natural gas [13]. In this study, proximate and ultimate analysis data for the natural gas used in the 880 MW CCPP operated by PT. X is obtained through a weighted average of the measurements taken throughout the year 2024, using Eq. (2).

$$\text{Weighted Average} = \frac{\sum(\text{Percentage of component}_i \times \text{Monthly gas usage}_i)}{\text{Total annual gas usage}} \quad (2)$$

The weighted average calculation considers the fuel consumption weight during each measurement period, ensuring that the result accurately reflects the actual fuel usage. Table 1 shows the annual

gas usage data in the weighted average calculation. Based on the measurements in Table 2, the main component in natural gas is Methane (CH₄), which has the highest molar content at 96.596%.

This is consistent with the typical characteristics of natural gas, where CH₄ is the dominant component in natural hydrocarbon mixtures [17].

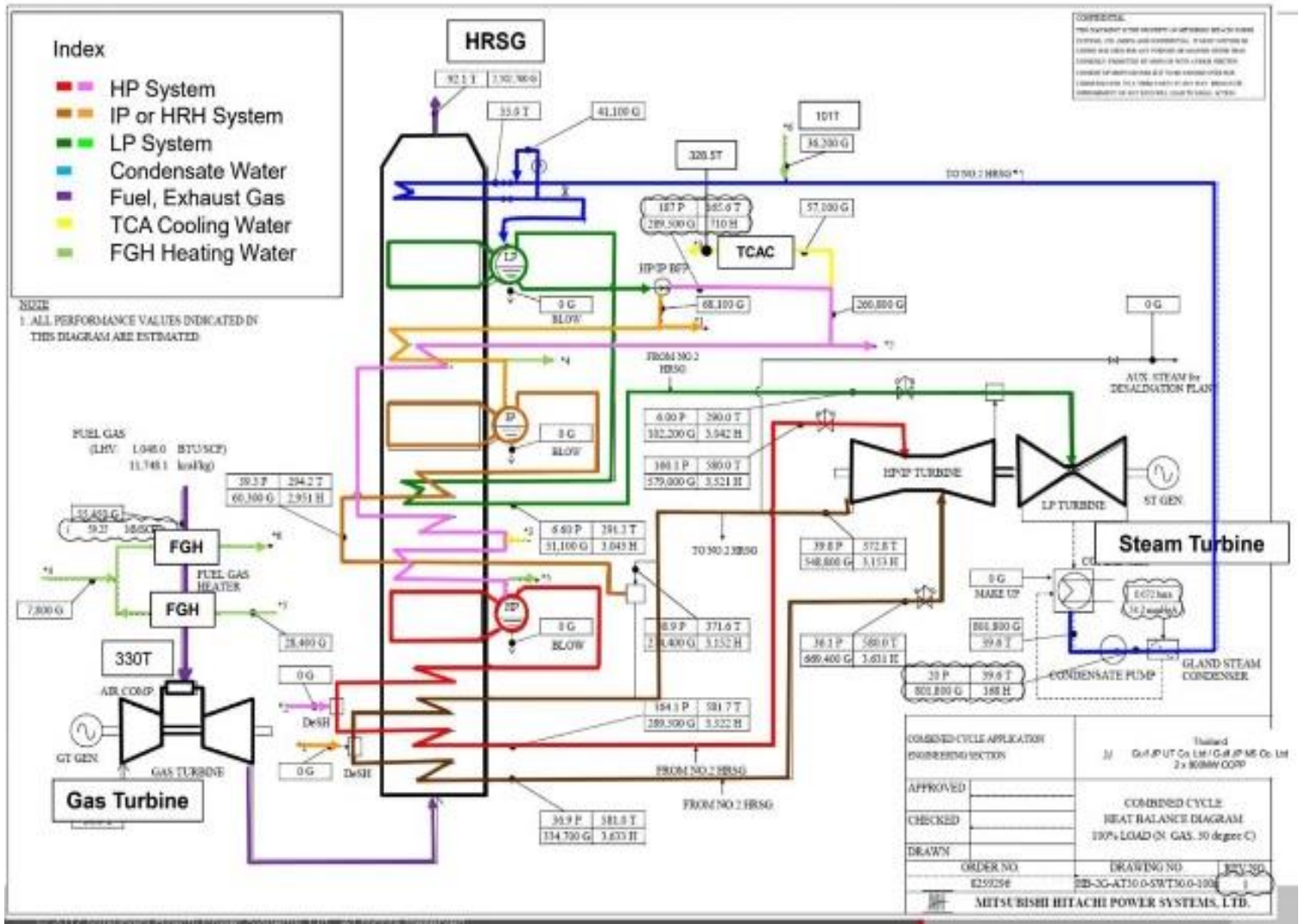


Fig. 1. Schematic of triple-pressure reheat CCGT power plant

Table 2. Weighted average calculation of natural gas measurements for 2024

Parameter	Unit	Jan	Feb	Mar	Apr	May	Jun	Jul	Aug	Sep	Oct	Nov	Des	Weighed average
Gas Composition														
CH ₄ (C1)	% Mol	96.6266	96.5450	96.4960	96.5220	96.4289	96.5560	96.5448	96.5154	96.5214	96.8576	96.7116	96.7264	96.596
Ethane (C2)	% Mol	2.3990	2.3450	2.3350	2.5420	2.5589	2.4280	2.4194	2.4289	2.4344	2.0860	2.2327	2.2273	2.356
Propane (C3)	% Mol	0.5396	0.5936	0.4670	0.5640	0.5892	0.5490	0.5548	0.5694	0.5514	0.4423	0.4614	0.4602	0.525
i-Butane (iC4)	% Mol	0.0621	0.0655	0.0870	0.1040	0.1167	0.1020	0.1056	0.1124	0.1101	0.0868	0.0814	0.0812	0.092
n-Butane (nC4)	% Mol	0.0354	0.0721	0.1070	0.1190	0.1205	0.1240	0.1286	0.1324	0.1286	0.1150	0.1010	0.1007	0.107
i-Pentane (iC5)	% Mol	0.0450	0.0240	0.0500	0.020	0.0279	0.0190	0.0214	0.0201	0.0246	0.0659	0.0331	0.0330	0.033
n-Pentane (nC5)	% Mol	0.0131	0.0142	0.0440	0.0030	0.0054	0.0140	0.0168	0.0124	0.0138	0.0450	0.0239	0.0238	0.020
Hexanes (C6)	% Mol	0.0390	0.0211	0.0520	0.0010	0.0033	0	0	0	0	0.0209	0.0276	0.0275	0.017
Heptanes plus (C7+)	% Mol	0	0.0769	0.0990	0	0	0	0	0	0	0.0381	0.0553	0.0551	0.029
N ₂	% Mol													
CO ₂	% Mol	0.2270	0.2324	0.2510	0.1120	0.1136	0.2010	0.2002	0.2012	0.2094	0.2395	0.2640	0.2559	0.215
H ₂ S	% Mol	0.0132	0.0102	0.0140	0.0130	0.0356	0.0070	0.0084	0.0078	0.0063	0.0029	0.0080	0.0089	0.010
Total	% Mol	0	0	0	0	0	0	0	0	0	0	0	0	-
Additional		100	100	100	100	100	100	100	100	100	100	100	100	100
Sp. Gravity Gas	-													-
Ideal GCV (@14.73 psi, 60 F)	BTU/ft ³	0.5768	0.5776	0.5797	0.5759	0.5706	0.5746	0.5846	0.5772	0.5808	0.5745	0.5786	0.5741	0.577

Inert components such as N₂ and CO₂ in natural gas are found in small molar fractions, at 0.215% and 0.010%, respectively. This composition aligns with research showing that natural gas often contains small amounts of inert gases that can affect the fuel's calorific value and combustion quality [18].

Additionally, the absence of Hydrogen Sulfide (H₂S) in the analyzed natural gas composition indicates that this gas has very low or undetectable sulfur content. According to the literature, natural gas that does not contain H₂S is classified as "sweet gas," meaning it is cleaner and does not require complex purification processes before being used in industry. The low sulfur content in natural gas helps reduce the risk of corrosion in pipeline infrastructure and decreases

harmful SO₂ emissions that are detrimental to the environment [19]. Therefore, the natural gas analyzed in this study has good combustion quality due to its low levels of contaminants such as CO₂ and H₂S, making it more efficient for use in the energy and industrial sectors.

3.2 Carbon content calculation

The calculation determines the total carbon content in the natural gas fuel used in the CCGT. This value is the basis for estimating the CO₂ emissions produced during the combustion process. The carbon content is determined based on the molar fraction of each hydrocarbon component present in the natural gas fuel. Each

hydrocarbon compound has a different number of carbon atoms, contributing to the total carbon in the fuel gas mixture [20]. In this study, the carbon content of the natural gas fuel is calculated based on the gas composition data obtained from Table 2.

In the carbon content calculation, the values for the Carbon Component and Total Components are obtained from the relative

atomic values of each element in the fuel components. The relative atomic values of carbon, hydrogen, oxygen, and N₂ in the hydrocarbon compounds are used to determine the contribution of each component to the total carbon in the gas mixture [21]. The carbon content results for each fuel component are shown in the following Table 3.

Table 3. Carbon content calculation

Gas	Chemical formula	%	Relative atomic weight				Molecular weight				C component	Total components	
			C	H	O	N	C	H	O	N			Total
CH ₄	CH ₄	96.5963	12	1	0	0	12	4	0	0	16	1159.155424	1545.540565
N ₂	N ₂	0.2148	0	0	0	14	0	0	0	28	28	0	6.014546053
Carbon dioxide	CO ₂	0.0103	12	0	16	0	12	0	32	0	44	0.123805269	0.453952653
Ethane	C ₂ H ₆	2.3565	12	1	0	0	24	6	0	0	30	56.55482361	70.69352951
Propane	C ₃ H ₈	0.5247	12	1	0	0	36	8	0	0	44	18.8897108	23.08742431
i-Butane	C ₄ H ₁₀	0.0919	12	1	0	0	48	10	0	0	58	4.412950044	5.332314636
n-Butane	C ₄ H ₁₀	0.1067	12	1	0	0	48	10	0	0	58	5.121847728	6.188899338
i-Pentane	C ₅ H ₁₂	0.0327	12	1	0	0	60	12	0	0	72	1.9634	2.356096498
n-Pentane	C ₅ H ₁₂	0.0203	12	1	0	0	60	12	0	0	72	1.215424915	1.458509898
n-Hexane	C ₆ H ₁₄	0.0169	12	1	0	0	72	14	0	0	86	1.213611952	1.449592054
n-Octane	C ₈ H ₁₈	0.0000	12	1	0	0	96	18	0	0	114	0	0
C ₆₊	C ₆₊	0.0000	12	0	0	0	72	0	0	0	72	0	0
n-heptane	C ₇ H ₁₆	0.0289	12	1	0	0	84	16	0	0	100	2.431734336	2.894921829
Total		100.000									Total	1251	1665
												Carbon Content	75.12%

Based on the calculation results, the total carbon component in the natural gas fuel used is 1251 units, while the total components in the gas mixture amount to 1665 units. This comparison shows that carbon dominates the fuel composition, making it a key factor in estimating the CO₂ emissions produced during combustion. By comparing the total carbon to the overall components in natural gas, the carbon content is found to be 75.12%, reflecting the characteristics of a fuel with high combustion efficiency.

The natural gas analyzed shows a carbon content of 75.12%, which is within the typical range for natural gas. According to Dittl and Sulc, the carbon content in natural gas typically varies between 75% and 90%, depending on the specific hydrocarbon composition [21]. The variation in carbon content is influenced by the types and proportions of hydrocarbons present in the gas, which can be affected by factors such as the geological source, extraction methods, and the degree of processing the gas undergoes before it is analyzed. This data indicates that the analyzed gas falls within the expected range for natural gas.

3.3 NCV calculation

The approach used in this study's NCV calculation involves several key stages. The first stage is determining the gross fuel consumption, which is the total fuel used in the power plant system over a specified period. Next, the conversion to net consumption is made by considering the combustion efficiency and correction factors based on the fuel composition [22].

Furthermore, total gross fuel consumption is obtained by summing the gross consumption of each hydrocarbon component,

including CH₄, Ethane (C₂H₆), Propane (C₃H₈), Butane (C₄H₁₀), Pentane (C₅H₁₂), as well as inert gases such as N₂ and CO₂. The total gross consumption is calculated by multiplying the molar percentage of each component by the Gross Calorific Value (GCV) of the fuel [23]. After obtaining the total gross consumption, the next step is calculating the total net consumption by considering the correction factors used in the GPA Standard 2145-16, specifically the Table of Physical Properties for Hydrocarbons and Other Compounds of Interest to the Natural Gas Industry. This correction is performed by applying the constant factor difference between the GCV and NCV for each fuel component [20]. The constant difference values for each component are provided in Table 3.

After obtaining the total net consumption, the next step is to calculate the NCV in units of TJ/Gg. This calculation is done to facilitate emission estimation on an industrial scale. NCV is expressed in units of mass, so the result obtained in energy per volume units needs to be converted by dividing it by the fuel's density, which is provided in Table 2. All the results of the total gross consumption, net consumption, and NCV values for the fuel are presented in Table 4, which summarizes all the parameters used in the emission analysis for this study.

Based on the calculation results, the NCV of the natural gas used in this study is 49.233 MJ/kg. This value is higher than the standard NCV for commercial natural gas, typically around 47.1 MJ/kg [21]. This difference may be caused by variations in the hydrocarbon composition, particularly a CH₄ content or the presence of heavier hydrocarbons such as C₂H₆ and C₃H₈ in more significant amounts [17].

Table 4. NCV calculation for gas

Gas	Chemical formula	Volume	GCV (Btu/ft ³)	Correction factor	Difference	NCV (Btu/ft ³)	
CH ₄	CH ₄	0.96596	1000.02	0.0996	99.60	900.42	
N ₂	N ₂	0.00215	2.22	0.0000	-	2.22	
Carbon Dioxide	CO ₂	0.00010	0.11	0.0790	0.01	0.10	
Ethane	C ₂ H ₆	0.02356	24.40	0.0852	2.08	22.32	
Propane	C ₃ H ₈	0.00525	5.43	0.0799	0.43	5.00	
i-Butane	C ₄ H ₁₀	0.00092	0.95	0.0775	0.07	0.88	
n-Butane	C ₄ H ₁₀	0.00107	1.10	0.0770	0.09	1.02	
i-Pentane	C ₅ H ₁₂	0.00033	0.34	0.0755	0.03	0.31	
n-Pentane	C ₅ H ₁₂	0.00020	0.21	0.0753	0.02	0.19	
n-Hexane	C ₆ H ₁₄	0.00017	0.17	0.0740	0.01	0.16	
n-Octane	C ₈ H ₁₈	0.00000	0.00	0.0725	-	-	
C ₆₊	C ₆₊	0.00000	0.00	0.0000	-	-	
n-heptane	C ₇ H ₁₆	0.00029	0.30	0.0732	0.02	0.28	
Total		1.000				932.90	
						NCV (TJ/Gg)	49.233

Additionally, the difference in NCV values may also be associated with inert components such as N₂ and CO₂ in natural gas. Higher levels of N₂ and CO₂ in the gas mixture can reduce the net calorific value, as these gases do not contribute to combustion energy. Furthermore, the moisture content and other non-hydrocarbon compounds in natural gas can also impact the reduction in NCV, as these gases are non-combustible and only act as additional mass without providing energy. Therefore, natural gas with higher CO₂ and N₂ tends to have a lower calorific value [19]. Thus, the value of 49.233 MJ/kg obtained in this study indicates that the natural gas used has a composition richer in heavy hydrocarbons, contributing to a higher calorific value than the standard commercial natural gas.

3.4 CO₂ emission calculation

The CO₂ emissions calculation in this study aims to assess the impact of hydrogen and natural gas blending on GHG emissions in CCPP. The Tier-2 Method-2, as outlined in the IPCC Guidelines for National GHG Inventories [24], is used for this calculation. This method is suitable as the available data includes the NCV and carbon content of natural gas, with standard oxidation factors applied. Tier 3, which assumes unburned carbon, and Tier 4, using CEMS, are not applicable due to the complete combustion of natural gas in CCPP and limitations in CEMS data collection during open cycle operation.

For the 100% natural gas scenario, CO₂ emissions are calculated based on fuel consumption without hydrogen blending. Aspen Plus[®] modeling is used for hydrogen blending scenarios to simulate fuel mixture properties and calculate CO₂ emission reductions more accurately. This approach provides an estimate of CO₂ reductions in tons, helping evaluate the effectiveness of hydrogen co-firing. The total natural gas consumption is obtained from the plant's operational data, with carbon content calculations based on the fuel composition. The oxidation factor used is the default national factor as per the IPCC guidelines (Eq. (3)).

$$E_{CO_2} = F_{gas} \times 0.001015 \times \frac{C}{NCV} \times FO \times 10^3 \times 44/12 \quad (3)$$

Data used in Eq. (3) are Consumption gas (F_{gas}) is 34850213.42 MMBTU (Table 4), carbon content (C) is 75.12% (Table 3), NCV is 49233 TJ/Gg (Table 4), and oxidation factor (OF) is 100% (default nationwide).

$$E_{CO_2} = F_{gas} \times 0.001055 \times \frac{C}{NCV} \times FO \times 10^3 \times 44/12$$

$$E_{CO_2} = 34850213.42 \times 0.001015 \times \frac{75.12\%}{49.233} \times 100\% \times 10^3 \times \frac{44}{12}$$

$$E_{CO_2} = 34850213.42 \times 0.001015 \times 0.001525 \times 10^3 \times \frac{44}{12}$$

$$E_{CO_2} = 34850213.42 \times 0.05874$$

$$E_{CO_2} = 2047101.53 \text{ ton } CO_2$$

Thus, the final result of the CO₂ emission calculation for the 100% natural gas scenario is 2.047.101,53 tons of CO₂ per year at CCPP X. This emission value serves as a baseline for evaluating the environmental impact of using pure natural gas and as a comparison in the hydrogen co-firing scenario analysis, which aims to reduce CO₂ emissions and improve the operational sustainability of CCPP.

3.5 Model simulation

Based on the technical data obtained from the manufacturer, manuals, and operational specifications of the power generation system, a simulation model was created using Aspen Plus[®] software. Information such as turbine capacity, Air-to-Fuel Ratio (A/F ratio), pressure, temperature, and mass flow rates of each component was input as parameters to build a process model that represents the actual conditions of the power generation system [21]. This simulation aims to illustrate the thermodynamic flow comprehensively and evaluate the impact of hydrogen blending on the performance and emissions of the natural gas-fired power generation system. The flowsheet of the process model is shown in Fig. 2. The simulation was conducted using Aspen Plus[®] software to analyse the Performance and Emission Analysis of Hydrogen. The details of each operating condition for each device can be seen in Table 5.

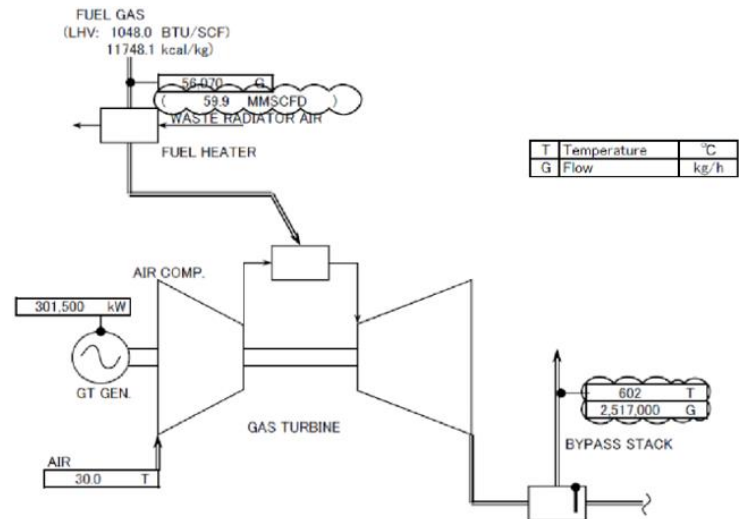


Fig. 2. Gas turbine open-cycle heat balance diagram

Table 5. Simulation equipment specifications

No	Name of component	Symbol/label	Main function	Process detail
1	Air intake	Air	Air resource	The air is compressed and prepared for combustion in the combustion chamber
2	Air filter	EXAIR	Air pre-heater	The air is filtered from dust particles, dirt, and contaminants before being compressed
3	Hydrogen inlet	H ₂	Additional fuel	Hydrogen is injected as an alternative or blended fuel into the combustion system
4	Natural gas inlet	NG	Main fuel	Natural gas enters as the primary fuel for combustion in the combustion chamber
5	Combustion chamber (Rgibbs)	OUTCOM	Combustion chamber	The mixing and combustion of air, natural gas, and hydrogen produce high-pressure hot gas
6	Gas turbine	TURBINE	Energy changer	The heat and pressure energy from the combustion gases is converted into mechanical energy (turbine rotation)
7	Exhaust gas out	EXHAUST	Exhaust gas	The residual combustion gases are released into the atmosphere or directed for further heat utilization
8	Chimney (cerobong)	CHIMNEY	Exhaust gas	Final gas disposal
9	Heat recovery steam generator (HRSG)	TURSTEAM	Residual heat	The heat from the exhaust gases is converted into steam for further processes or additional power generation
10	Steam turbine	OUT	Steam turbine	The steam energy is converted into additional mechanical power
11	Recycle line	RECYCLE	Steam recycle	A portion of the steam is returned for reuse in the system
12	Cooling system	TO COOL	Steam cooler	The remaining steam is cooled before being condensed or reused
13	Condenser	COOL	Condenser	The steam is condensed into liquid water for recycling
14	Economizer (air preheater)	ECONIZ	Residual heat	The residual heat from the exhaust gases is used to heat the boiler feedwater
15	Pompa air umpan	RR	Pump	The water pressure is increased to enter the boiler or HRSG again

3.6 The influence of fuel characteristics on the air-fuel ratio

In this model, hydrogen and natural gas proportions are calculated by considering the A/F Ratio, which is the ratio of fuel to air used in the combustion process, as obtained from the manual book according to Fig. 2. Based on Fig. 2, fuel gas flow is 56070

Kg/h, total flow mixture is 2517000 kg/h, and used air is 2517000 – 56070 = 2460930 kg/h, so it can be calculated using Eq. (4).

$$A/F \text{ Ratio} = \frac{\text{Air mass}}{\text{Fuel mass}} \quad (4)$$

$$\frac{A}{F} \text{ Ratio} = \frac{2460930}{56070} = 43.89$$

From these calculations, the A/F Ratio of 43.89 is used for the combustion process in the 100% natural gas scenario, indicating that this ratio represents the air-to-fuel requirement under initial operating conditions before being mixed with hydrogen.

In the hydrogen co-firing simulation for a Natural Gas Combined Cycle (NGCC) power plant (Fig. 3 and Table 5), it is observed that the A/F Ratio is not constant but changes progressively as the energy fraction of hydrogen (%) increases. This is shown by the simultaneous decrease in the mass flow rate of air and fuel, as listed in Table 4. However, the reduction in the mass flow rate of fuel occurs at a greater proportion than air, leading to an overall increase

in the A/F ratio. Technically, this phenomenon is closely related to the stoichiometric differences between methane (the main component of natural gas) and hydrogen as fuels.

The stoichiometric combustion reaction of methane requires about two moles of oxygen for every mole of CH₄, while hydrogen only requires half a mole of O₂ per mole of H₂. In other words, to produce the same power, using hydrogen as a fuel requires much less oxygen than methane. Hydrogen and natural gas (mainly methane, CH₄) have different combustion stoichiometries:

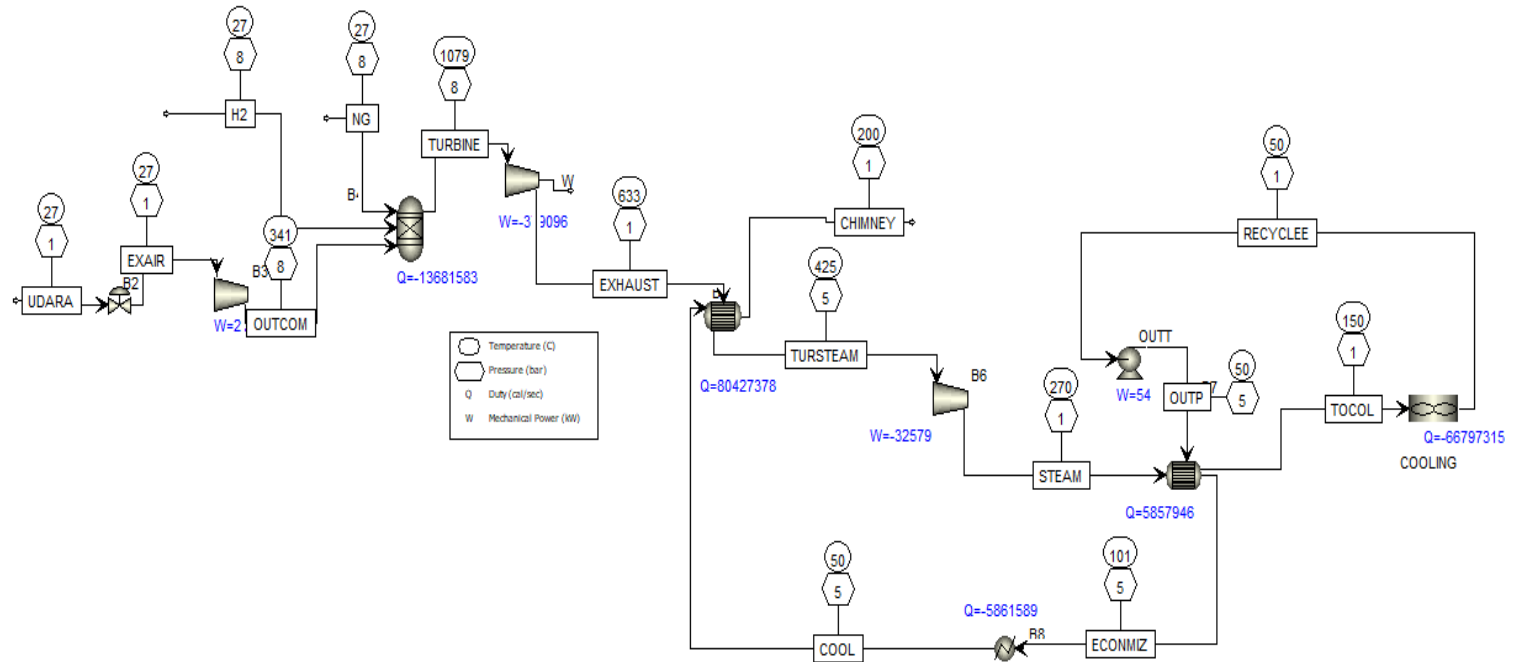
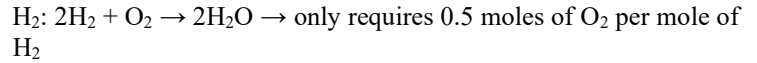
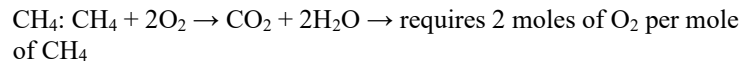


Fig. 3. Aspen Plus® simulation flowsheet of hydrogen and natural gas co-firing in a power plant

Thus, hydrogen requires much less O₂ per unit of energy than methane. This means that when hydrogen is added, the total air requirement for combustion decreases, even though the power output remains constant. Moreover, the higher calorific value of hydrogen (~120 MJ/kg) compared to methane (~50 MJ/kg) reduces the fuel mass needed, further lowering the system's total fuel mass flow rate. Additionally, changes in the A/F ratio are part of the system's effort to maintain combustion balance. In the gas turbine combustion process, the air-fuel mixture composition heavily influences flame stability, thermal efficiency, and emission levels. If the ratio is not adjusted to match the new fuel composition, the system risks incomplete combustion, high emissions (such as NO_x), or even flame instability. Therefore, the combustion control system automatically adjusts the air and fuel flow rates to maintain the combustion process within an optimal zone.

The adjustment of the air-fuel ratio in the hydrogen co-firing system is explained by Dittl and Sulc (2024), who state, "the air mass flow rate decreased with the increase of the hydrogen co-firing ratio, caused by the reduction of oxygen demand due to the use of hydrogen as fuel, which requires less oxygen than methane for complete combustion". This statement emphasizes that the change in the A/F ratio is not only due to the reduced oxygen demand caused by hydrogen's stoichiometric characteristics but also as part of the combustion control strategy to maintain stability, thermal efficiency, and overall system performance amid changes in fuel composition. Thus, the change in the A/F ratio in hydrogen co-firing in NGCC results from a combination of different stoichiometric combustion needs and the combustion control system working to maintain stability and thermal efficiency through the principle of combustion balance.

3.7 The influence of combustion system temperature

This study analyzes the impact of hydrogen co-firing on CO₂ and NO emissions at various combustion temperatures (Fig. 4). Based on the resulting graph, it is evident that hydrogen has a significant effect in reducing CO₂ emissions, but does not show a significant change in NO emissions. In the CO₂ vs. temperature graph, it is seen that the amount of CO₂ produced remains constant at each temperature for each hydrogen variation. However, as the percentage of hydrogen in the fuel mixture increases, CO₂ emissions decrease. [25]. In the absence of hydrogen (0% H₂), CO₂ emissions are 3499.26 KMOL/H, while with 10% H₂ they drop to 3149.33 KMOL/H, and further decrease to 2799.41 KMOL/H at 20% H₂. This aligns with hydrogen's characteristic as a carbon-free fuel, meaning the higher its usage, the lower the CO₂ formed [19].

On the other hand, the NO vs. temperature graph (Fig. 4) shows a drastic increase in NO emissions as the combustion temperature rises. At low temperatures around 300K, NO formation is minimal and almost zero. However, as the temperature rises to 800K, NO emissions start to increase, and at temperatures above 1050K, there is a significant spike, reaching over 77 KMOL/H at 1200K [19]. An interesting finding is that the percentage of hydrogen in the fuel does not significantly affect NO emissions, as the results are nearly identical for each hydrogen variation. This observation suggests that NO formation is more strongly influenced by high combustion temperatures than by hydrogen concentration. Breer et al. (2023) demonstrated this through simulations at constant flame temperatures, where NO emissions did not increase significantly with higher hydrogen content and, in some cases, even decreased. Specifically, they concluded that "given the strong temperature sensitivity of NO_x production, these comparisons were performed

at a constant flame temperature" and that "NO emissions monotonically decrease with increased H₂ fraction in premixed conditions when temperature is held constant" [26].

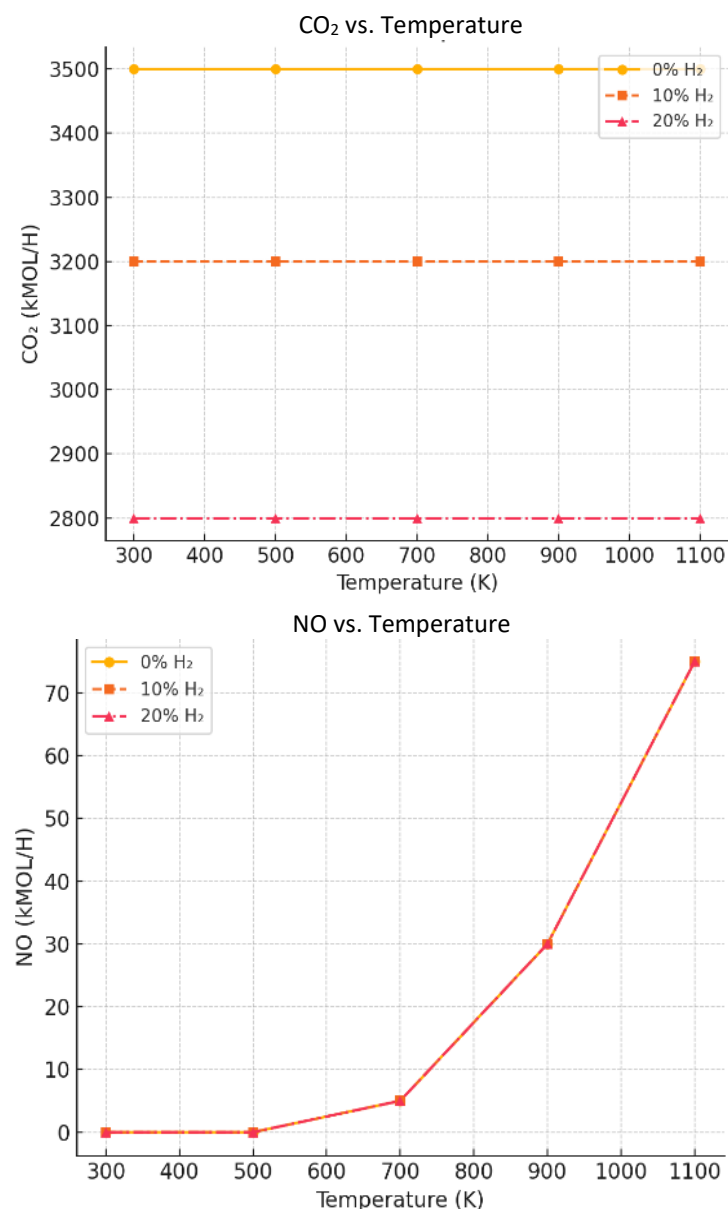


Fig. 4. The influence of hydrogen co-firing combustion system temperature

From these results, it can be concluded that hydrogen co-firing is very effective in reducing CO₂ emissions, making it a more environmentally friendly solution than pure fossil fuels. However, concerning NO_x emissions, the increase in temperature due to combustion remains the main factor determining the amount of NO formed. Therefore, to reduce NO_x emissions, additional methods such as combustion temperature control, the use of Flue Gas Recirculation (FGR), or the application of Selective Catalytic Reduction (SCR) technology are needed [27]. By understanding this pattern, hydrogen co-firing implementation can be optimized in reducing the environmental impact of carbon emissions and addressing the challenges of NO_x emissions that may rise due to high combustion temperature [17].

Based on the table of simulation results with the gas mixture characteristics and power plant performance with hydrogen co-firing variations of 0%, 10%, and 20%, it can be observed that there are significant trends of change in fuel consumption, power performance, efficiency, and environmental emissions. The application of hydrogen as an additional fuel directly affects the amount of primary fuel consumption, namely Natural Gas (NG), which decreases from 56.070 kg/hr at 0% H₂ to 44.856 kg/hr when the H₂ content reaches 20%. This decrease is due to some of the energy requirements being met by hydrogen, which has a higher

calorific value per unit mass compared to methane (the main component of NG), as explained by Sun et al., that the use of hydrogen can reduce dependence on fossil fuels while improving combustion performance [17].

Along with the decrease in NG consumption, the air mass flow rate used for the combustion process also decreases, from 2460930 kg/hr to 2424852 kg/hr. This is due to the lower oxygen demand as the fuel composition shifts towards hydrogen, which has a different combustion stoichiometric ratio than NG. Despite changes in the fuel mixture composition, the temperature (27°C) and pressure (8 bar) of the system are maintained to ensure the balance and stability of the combustion system operation.

However, adding hydrogen does not automatically increase the total electrical power generated. The power produced by the gas turbine decreases from 385.90 MW to 379.09 MW, and the power from the steam turbine also drops from 34.39 MW to 32.57 MW. This indicates that despite the increased energy content in the fuel mixture, the total fuel mass flow decreases, resulting in a reduction in the total energy entering the system. This phenomenon aligns with findings explained by Duchowny et al., where hydrogen co-firing in gas turbines can reduce the total energy supply if not balanced by adjustments in fuel flow rates [24].

Although the total output power tends to decrease, the thermal efficiency of the system experiences a significant increase. Under baseline conditions (0% H₂), the system efficiency is recorded at 53.96%, and increases to 56.76% at 10% H₂, even reaching 59.96% at 20% H₂. This increase in efficiency is consistent with the theory that hydrogen has faster and cleaner combustion characteristics, thus resulting in more efficient energy conversion processes [28]. Therefore, despite the decrease in power, the energy used to generate that power becomes more optimal and efficient.

From an environmental perspective, the use of hydrogen proves to be highly effective in drastically reducing CO₂ emissions. Under initial conditions without hydrogen, CO₂ emissions reach 154001.74 kg/hr, but decrease to 123201.39 kg/hr at 20% H₂ co-firing. This is consistent with hydrogen combustion not producing carbon, so substituting part of the NG with H₂ directly reduces total CO₂ emissions (IEA, 2019). Therefore, this strategy is highly relevant in supporting the decarbonization goals of power plants [29].

However, there are consequences for nitrogen oxide (NO) emissions, which show a slight increase from 1197.88 kg/hr without H₂ to 1.223174 kg/hr at 20% H₂. The increase in NO_x emissions is related to hydrogen's high combustion temperature, which triggers thermal-NO_x formation[30]. Therefore, implementing NO_x mitigation technologies, such as SCR, should be considered in H₂ co-firing-based power systems.

Additionally, the fuel mixture's Lower Heating Value (LHV) also increases with the percentage of H₂, from 0.023256 MJ/kg to 0.024222 MJ/kg. This indicates that each kilogram of the fuel mixture now contains more energy due to the contribution of H₂, which has a higher LHV than methane.

Overall, from this analysis, it can be concluded that the implementation of up to 20% H₂ co-firing can significantly increase the thermal efficiency of the system and reduce CO₂ emissions. However, attention must be paid to the potential increase in NO_x emissions and the decrease in electrical power generated. Therefore, the H₂ co-firing strategy in natural gas-based power plants represents one of the energy transition solutions towards a cleaner and more efficient system.

3.8 Comparison of simulation and design

Table 6 shows the comparison between the simulation results and design data for three key parameters in a gas turbine-based power generation system: the LHV of natural gas, the net output power of the gas turbine, and the flue gas temperature at low-pressure (LP) steam. The simulation results indicate an LHV value of 49.65 MJ/kg, while the design value is 54.54 MJ/kg, resulting in a relative error of 9.848%. This deviation is quite significant and is likely due to differences in the composition and density of the natural gas used in

the simulation compared to the actual design data during equipment commissioning.

Table 6. Comparison of simulation and design

Parameter	Simulation	Design	Relative error
LHV natural gas (MJ/kg)	49.65	54.54	9.848
Wnet gas turbine (kW)	421181	420000	0.238
Flue gas LP steam temperature (°C)	285	290	1.724
Temperature exhaust (°C)	635	615	3.252

When comparing the LHV value calculated based on the fuel composition data input into the simulation, it aligns with the value in Table 6, which is 49.233 MJ/kg. The LHV value from the Aspen simulation is 49.65 MJ/kg, yielding a relative error of just 0.84%. This slight deviation suggests that the fuel composition and density inputs used in the simulation adequately represent the actual conditions.

The net power output of the gas turbine in the simulation is 421.181 kW, which is very close to the design value of 420000 kW, with a relative error of only 0.238%. This slight difference demonstrates that the simulation model accurately represents the turbine's performance. Meanwhile, the flue gas temperature at LP steam from the simulation is 285°C, slightly lower than the design value of 290°C, resulting in a relative error of 1,724%. This minor deviation may be attributed to assumptions in heat transfer efficiency or operational conditions not fully captured in the simulation. The simulation records a value of 635°C for the exhaust gas temperature, compared to 615°C in the design data, with a relative error of 3,252%. Such discrepancies can arise from simplifications in the model or from differences in operational settings during simulation and actual plant operation.

Although some deviations exist between simulation and design values, most of the results fall within an acceptable technical tolerance, as simulation errors below 5% are generally considered satisfactory for model validation in power plant studies [31]. These findings indicate that the simulation provides a sufficiently accurate representation of real plant conditions and can be considered reliable for further analysis of system performance and emission impacts.

3.9 Emission analysis at 10% and 20% hydrogen

Based on the simulation results in Table 7, CO₂ emissions decrease as the percentage of hydrogen in the fuel mixture increases. In the 10% hydrogen scenario, CO₂ emissions decrease by 10%, equivalent to 240469.44 tons/year, while in the 20% hydrogen scenario, the reduction reaches 20%, or 409.420,30 tons/year, based on the initial CO₂ emission calculation of 2047101.53 tons CO₂/year. These annual values were calculated using an operational assumption of 7800 hours per year in 2024 for a single gas turbine unit, which reflects typical plant availability and operating conditions in the Indonesian context. This decrease aligns with the characteristics of hydrogen, which contains no carbon. It thus does not produce CO₂ when burned, unlike natural gas, which is primarily composed of hydrocarbons such as CH₄. This finding is further supported by the study of Wang et al., which states that hydrogen blending can reduce CO₂ emissions by up to 6% for every 5% increase in hydrogen content in the fuel [32]. Conversely, NO emissions show an increasing trend. In the 10% hydrogen scenario, NO emissions increase by 13.13 kg/hr, or 1.10%, and at 20% hydrogen, they rise to 25.86 kg/hr, or 2.16% compared to the baseline. This is due to the higher combustion temperature resulting from hydrogen's reactive nature, accelerating the reaction and increasing thermal NO_x formation. This phenomenon is consistent with literature stating that increasing hydrogen content in the fuel mixture can enhance the concentration of O and OH radicals, which accelerate NO formation [33]. Thus, while hydrogen co-firing is highly effective in reducing CO₂ emissions, extra attention must be given to controlling NO_x emissions to ensure the overall environmental benefits remain intact [34]. In addition, the Lower Heating Value (LHV) of the fuel mixture increases with the percentage of H₂, from 0.023256 MJ/kg to 0.024222 MJ/kg, indicating that each kilogram of the fuel mixture contains more

energy due to the contribution of H₂, which has a higher LHV compared to methane.

Table 7. Effect of hydrogen co-firing on performance and emissions

Parameter	0%(Baseline)	10% (H ₂)	20% (H ₂)
CO ₂ emission (kg/hr)	154001.74	13860.57	123201.39
NO emission (kg/hr)	119788	1211.01	1223.74
LHV mass basis (MJ/kg)	0.023256	0.023736	0.024222
Gas turbine power (MW)	385.90	382.50	379.09
High-pressure steam turbine (MW)	12.34	12,00	11,66
Low-pressure steam turbine power (MW)	22.93	22.29	21.65
Total power output (MW)	421.17	416.79	412.67
Fuel energy input (MW)	778.75	732.71	686.67
Thermal efficiency	54.08%	56.88%	60.06%

The simulation also shows that increasing the hydrogen content results in a decrease in the net power output. The total power output drops from 421.17 MW at 0% hydrogen to 416.79 MW at 10% hydrogen and to 412.67 MW at 20% hydrogen. This reduction is primarily attributed to the lower overall mass flow rate and differences in combustion characteristics between hydrogen and methane.

Similarly, the fuel energy input decreases significantly as hydrogen content increases, from 778.75 MW in the baseline scenario to 732.71 MW at 10% hydrogen and 686.67 MW at 20% hydrogen. This demonstrates improved energy utilization as hydrogen is introduced.

Most notably, the plant's thermal efficiency increases with the percentage of hydrogen in the fuel mixture, from 54.08% at baseline to 56.88% at 10% hydrogen, and up to 60.06% at 20% hydrogen. This improvement is due to cleaner combustion and better energy conversion associated with hydrogen co-firing.

As shown in Fig. 5, the implementation of hydrogen co-firing up to 20% can significantly improve thermal efficiency and reduce CO₂ emissions. However, it must be balanced with careful attention to the potential increase in NO_x emissions and the decrease in net electricity output. Therefore, the hydrogen co-firing strategy in natural gas-based power plants represents an important energy transition solution toward a cleaner and more efficient system [33].

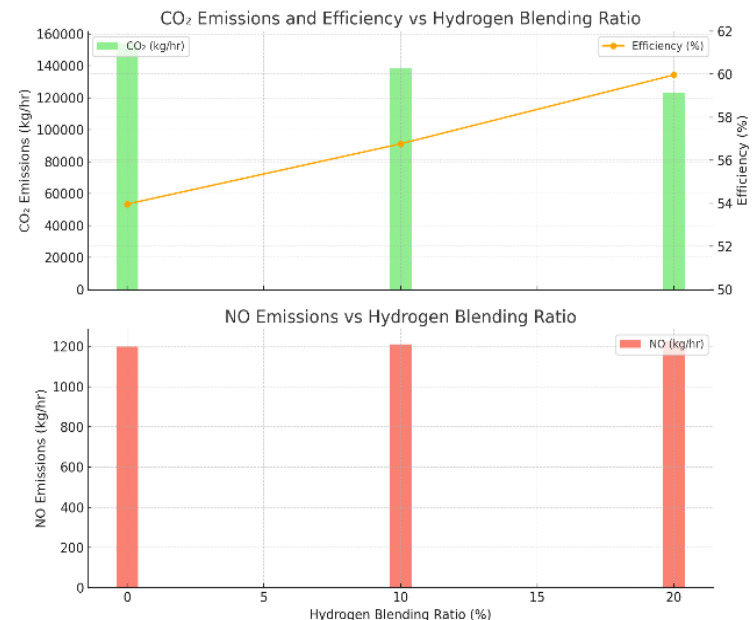


Fig. 5. The effect of hydrogen composition on efficiency, CO₂, and NO

4 Conclusion

This study demonstrates that hydrogen co-firing in a natural gas-fired 880 MW Combined Cycle Power Plant can deliver substantial reductions in CO₂ emissions while simultaneously improving thermal efficiency. The Aspen Plus simulations indicate a clear proportional relationship between hydrogen content in the fuel mixture and CO₂ reduction.

- The emissions decreased from 15,401.74 kg/hr under the baseline condition to 13,860.16 kg/hr at a 10% hydrogen blend and 12,320.14 kg/hr at a 20% hydrogen blend. This translates to an annual reduction of approximately 409,420 tons of CO₂, underscoring the effectiveness of hydrogen as a carbon-free energy carrier compared to natural gas, which is predominantly methane. In addition to emission benefits, hydrogen co-firing enhances energy conversion efficiency.
- Thermal efficiency improved from 54.08% at baseline to 56.88% and 60.06% with 10% and 20% hydrogen, respectively. These improvements confirm hydrogen's capacity to optimize fuel utilization in combined cycle configurations. However, these gains were accompanied by a modest decline in net power output, falling from 421.17 MW at 0% hydrogen to 416.79 MW and 412.67 MW at 10% and 20% hydrogen, respectively. This reduction is primarily attributed to differences in the fuel's calorific value and mass flow behavior.
- About environmental trade-offs, NO_x emissions increased slightly, rising from 1,197.88 kg/hr to 1,223.74 kg/hr (about 2.16%) at 20% hydrogen. Despite this increase, the resulting concentration of approximately 60 mg/Nm³ remains well below Indonesia's regulatory threshold of 400 mg/Nm³, suggesting that hydrogen co-firing can be implemented safely within current environmental standards. It is important to acknowledge that this study is based on steady-state simulations and does not capture transient dynamics or operational challenges that may arise in practice. Nevertheless, the inclusion of actual plant data for the baseline condition strengthens the credibility of the model.

Hydrogen co-firing represents a promising transitional solution to achieve meaningful CO₂ reductions and improved energy efficiency in power generation, with minimal environmental trade-offs. With proper emission management and further research, this technology can strategically support national and global decarbonization goals.

Reference

- [1] T. N. Zahari and B. C. McLellan, "Review of policies for Indonesia's electricity sector transition and qualitative evaluation of impacts and influences using a conceptual dynamic model," *Energies (Basel)*, vol. 16, no. 8, p. 3406, Apr. 2023, doi: 10.3390/en16083406.
- [2] N. A. Pambudi *et al.*, "Renewable energy in Indonesia: current status, potential, and future development," *Sustainability*, vol. 15, no. 3, p. 2342, Jan. 2023, doi: 10.3390/su15032342.
- [3] H. Wahyudi, "The Relationship between the renewable energy and CO₂ emissions to the Indonesian economy," *International Journal of Energy Economics and Policy*, vol. 14, no. 3, pp. 349–357, May 2024, doi: 10.32479/ijeeep.15903.
- [4] A. Farabi, Z. Zamroni, D. O. D. Handayani, and R. H. Setianto, "Sustainable development in Indonesia: A Study of energy consumption, CO₂ Emissions, FDI, and Gross Capital Formation," *International Journal of Energy Economics and Policy*, vol. 14, no. 2, pp. 435–446, Mar. 2024, doi: 10.32479/ijeeep.15424.
- [5] G. M. Idroes, I. Hardi, Md. H. Rahman, M. Afjal, T. R. Noviandy, and R. Idroes, "The dynamic impact of non-renewable and renewable energy on carbon dioxide emissions and ecological footprint in Indonesia," *Carbon Research*, vol. 3, no. 1, p. 35, Apr. 2024, doi: 10.1007/s44246-024-00117-0.
- [6] A. Massagony and Budiono, "Is the Environmental Kuznets Curve (EKC) hypothesis valid on CO₂ emissions in Indonesia?," *International Journal of Environmental Studies*, vol. 80, no. 1, pp. 20–31, Jan. 2023, doi: 10.1080/00207233.2022.2029097.
- [7] R. Kurniawan, G. P. Trencher, A. S. Edianto, I. E. Setiawan, and K. Matsubae, "Understanding the multi-faceted drivers of increasing coal consumption in Indonesia," *Energies (Basel)*, vol. 13, no. 14, p. 3660, Jul. 2020, doi: 10.3390/en13143660.
- [8] I. Kulušić, L. Jukić, I. Smajla, and D. Karasalihović Sedlar, "The Role of natural gas in the socio-technical transition to a carbon-neutral society and a review of the European Union's framework," *Sustainability*, vol. 16, no. 9, p. 3791, Apr. 2024, doi: 10.3390/su16093791.
- [9] D. Guilbert and G. Vitale, "Hydrogen as a clean and sustainable energy vector for global transition from fossil-based to zero-carbon," *Clean Technologies*, vol. 3, no. 4, pp. 881–909, Dec. 2021, doi: 10.3390/cleantechnol3040051.
- [10] J. Kleperis *et al.*, "Analysis of the role of the Latvian Natural gas network for the use of future energy systems: Hydrogen from Res," *Latvian Journal of Physics and Technical Sciences*, vol. 58, no. 3, pp. 214–226, Jun. 2021, doi: 10.2478/lpts-2021-0027.
- [11] M. Rieksta, E. Zarins, and G. Bazbauers, "Potential role of green hydrogen in decarbonization of district heating systems: A review," *Environmental and Climate Technologies*, vol. 27, no. 1, pp. 545–558, Jan. 2023, doi: 10.2478/rtuct-2023-0040.
- [12] R. Sitanggang, "Performance and emission analysis of hydrogen and natural gas co-firing in combined cycle gas turbine power generation," *Journal of Applied Engineering Science*, vol. 21, no. 2, pp. 678–685, 2023, doi: 10.5937/jaes0-41926.
- [13] D. Pashchenko, "Hydrogen-rich gas as a fuel for the gas turbines: A pathway to lower CO₂ emission," *Renewable and Sustainable Energy Reviews*, vol. 173, p. 113117, Mar. 2023, doi: 10.1016/j.rser.2022.113117.
- [14] Z. Abdin, "Bridging the energy future: The role and potential of hydrogen co-firing with natural gas," *J Clean Prod*, vol. 436, p. 140724, Jan. 2024, doi: 10.1016/j.jclepro.2024.140724.
- [15] K. Bąk, P. Ziółkowski, J. Frost, and M. Drosińska-Komor, "Comparative study of a combined heat and power plant retrofitted by CO₂ capture during the combustion of syngas from sewage sludge gasification versus zero-emission combustion of hydrogen produced using renewables," *International Journal of Hydrogen Energy*, vol. 48, no. 99, pp. 39625–39640, Dec. 2023, doi: https://doi.org/10.1016/j.ijhydene.2023.07.322.
- [16] J. C. Hower, R. B. Finkelman, C. F. Eble, and B. J. Arnold, "Understanding coal quality and the critical importance of comprehensive coal analyses," *Int J Coal Geol*, vol. 263, p. 104120, Nov. 2022, doi: 10.1016/j.coal.2022.104120.
- [17] H. Sun, R. Li, M. Huang, Z. Li, and J. Xu, "Numerical simulations of the influence of inert gases (N₂/CO₂) on combustion characteristics of laminar-premixed biosyngas flame," *ACS Omega*, vol. 6, no. 22, pp. 14585–14597, Jun. 2021, doi: 10.1021/acsomega.1c01729.
- [18] C. Park, S. Oh, C. Kim, Y. Choi, and Y. Ha, "Effect of natural gas composition and gas interchangeability on performance and emission characteristics in an air–fuel controlled natural gas engine," *Fuel*, vol. 287, p. 119501, Mar. 2021, doi: https://doi.org/10.1016/j.fuel.2020.119501.
- [19] I. Hudák, P. Skryja, J. Bojanovský, Z. Jegla, and M. Krňávek, "The Effect of inert fuel compounds on flame characteristics," *Energies (Basel)*, vol. 15, no. 1, p. 262, Dec. 2021, doi: 10.3390/en15010262.
- [20] P. Divekar, X. Han, X. Zhang, M. Zheng, and J. Tjong, "Energy efficiency improvements and CO₂ emission reduction by CNG use in medium- and heavy-duty spark-ignition engines," *Energy*, vol. 263, p. 125769, Jan. 2023, doi: 10.1016/j.energy.2022.125769.

- [21] P. Ditzl and R. Šulc, "Calculations of CO₂ emission and combustion efficiency for various fuels," *Energy*, vol. 290, p. 130044, Mar. 2024, doi: 10.1016/j.energy.2023.130044.
- [22] E. H. de Paulo *et al.*, "Determination of gross calorific value in crude oil by variable selection methods applied to ¹³C NMR spectroscopy," *Fuel*, vol. 311, p. 122527, Mar. 2022, doi: 10.1016/j.fuel.2021.122527.
- [23] L. Vilakazi and D. Madyira, "Estimation of gross calorific value of coal: A literature review," *International Journal of Coal Preparation and Utilization*, vol. 45, no. 2, pp. 390–404, Feb. 2025, doi: 10.1080/19392699.2024.2339340.
- [24] A. Duchowny *et al.*, "Composition analysis of natural gas by combined benchtop NMR spectroscopy and mechanistical multivariate regression," *Energy Reports*, vol. 8, pp. 3661–3670, Nov. 2022, doi: 10.1016/j.egy.2022.02.289.
- [25] M. Ozturk, F. Sorgulu, N. Javani, and I. Dincer, "An experimental study on the environmental impact of hydrogen and natural gas blend burning," *Chemosphere*, vol. 329, p. 138671, Jul. 2023, doi: <https://doi.org/10.1016/j.chemosphere.2023.138671>.
- [26] B. Breer *et al.*, "Numerical investigation of NO_x production from premixed hydrogen/methane fuel blends," *Combustion and Flame*, vol. 255, p. 112920, Sep. 2023, doi: <https://doi.org/10.1016/j.combustflame.2023.112920>.
- [27] S. Park, J. Shin, J. Park, S. Lee, and N. Choi, "Comparison of hydrogen and ammonia co-firing with natural gas using a practical gas turbine combustor (501F) under atmospheric conditions: changes in metal temperature, pattern factor, and NO_x emission," Jun. 2023, doi: <https://doi.org/10.1115/gt2023-103364>.
- [28] D. Cecere, E. Giacomazzi, A. Di Nardo, and G. Calchetti, "Gas turbine combustion technologies for hydrogen blends," *Energies (Basel)*, vol. 16, no. 19, p. 6829, Sep. 2023, doi: 10.3390/en16196829.
- [29] Y. Xu, H. Wang, X. Liu, J. Zhu, J. Xu, and M. Xu, "Mitigating CO₂ emission in pulverized coal-fired power plant via co-firing ammonia: A simulation study of flue gas streams and exergy efficiency," *Energy Convers Manag*, vol. 256, p. 115328, Mar. 2022, doi: 10.1016/j.enconman.2022.115328.
- [30] V. M. Maestre, A. Ortiz, and I. Ortiz, "Challenges and prospects of renewable hydrogen-based strategies for full decarbonization of stationary power applications," *Renewable and Sustainable Energy Reviews*, vol. 152, p. 111628, Dec. 2021, doi: 10.1016/j.rser.2021.111628.
- [31] B. Faqih and F. Ghaith, "A comprehensive review and evaluation of heat recovery methods from gas turbine exhaust systems," *International Journal of Thermofluids*, vol. 18, p. 100347, May 2023, doi: <https://doi.org/10.1016/j.ijft.2023.100347>.
- [32] T. Wang, H. Zhang, Y. Zhang, H. Wang, J. Lyu, and G. Yue, "Efficiency and emissions of gas-fired industrial boiler fueled with hydrogen-enriched nature gas: A case study of 108 t/h steam boiler," *Int J Hydrogen Energy*, vol. 47, no. 65, pp. 28188–28203, Jul. 2022, doi: 10.1016/j.ijhydene.2022.06.121.
- [33] N. Skordoulias, E. I. Koytsoumpa, and S. Karellas, "Techno-economic evaluation of medium scale power to hydrogen to combined heat and power generation systems," *Int J Hydrogen Energy*, vol. 47, no. 63, pp. 26871–26890, Jul. 2022, doi: 10.1016/j.ijhydene.2022.06.057.
- [34] S. Molina, S. Ruiz, J. Gomez-Soriano, and M. Olcina-Girona, "Impact of hydrogen substitution for stable lean operation on spark ignition engines fueled by compressed natural gas," *Results in Engineering*, vol. 17, p. 100799, Mar. 2023, doi: 10.1016/j.rineng.2022.100799.